

1 **Prompt apoptotic response to high glucose in SGLT expressing renal cells**

2 Linnéa M. Nilsson¹, Liang Zhang², Alexander Bondar³, Daniel Svensson², Annika
3 Wernerson⁴, Hjalmar Brismar^{1,2}, Lena Scott², Anita Aperia²

4

5 ¹Science for Life Laboratory, Department of Applied Physics, Royal Institute of
6 Technology, Solna, Sweden

7 ²Science for Life Laboratory, Department of Women's and Children's Health,
8 Karolinska Institutet, Solna, Sweden

9 ³Institute of Chemical Biology and Fundamental Medicine, Novosibirsk, Russia

10 ⁴Division of Renal Medicine, Department of Clinical Science, Intervention and
11 Technology, Karolinska Institutet, Stockholm, Sweden

12

13 Running head

14 Glucose toxicity in SGLT expressing cells

15

16 Address for Correspondence

17 Anita Aperia

18 Science for Life Laboratory

19 Box 1031

20 171 21 Solna, Sweden

21 Email: anita.aperia@ki.se

22

23 Author Contributions

24 L.N. performed experiments, analyzed data, wrote manuscript. L.Z. performed
25 experiments, analyzed data. A.B. designed PCR experiments. D.S. performed
26 experiments, analyzed data. A.W. analyzed clinical data. H.B. designed study,
27 reviewed and edited manuscript. L.S. designed study, analyzed data, reviewed and
28 edited manuscript. A.A. designed study, wrote manuscript.

29 **ABSTRACT**

30 It is generally believed that cells that are unable to downregulate glucose transport
31 are particularly vulnerable to hyperglycemia. Yet little is known about the relation
32 between expression of glucose transporters and acute toxic effects of high glucose
33 exposure.

34 Here we have, in an ex vivo study on rat renal cells, compared the apoptotic
35 response to a moderate increase in glucose concentration. We have studied the cell
36 types that commonly are targeted in diabetic kidney disease (DKD): proximal tubule
37 cells (PTC) that express SGLT2, mesangial cells (MC) that express SGLT1, and
38 podocytes that lack SGLT and take up glucose via the insulin dependent GLUT4.

39 PTC and MC responded within 4-8 h exposure to 15 mM glucose with translocation
40 of the apoptotic protein Bax to mitochondria and increased apoptotic index. SGLT
41 down-regulation and exposure to SGLT inhibitors abolished the apoptotic response.
42 Onset of overt DKD generally coincides with onset of albuminuria. Albumin had an
43 additive effect on the apoptotic response. Ouabain, which interferes with apoptotic
44 onset, rescued from the apoptotic response. Insulin supplemented podocytes
45 remained resistant to 15 and 30 mM glucose for at least 24 h.

46 Our study points to a previously unappreciated role of SGLT dependent glucose
47 uptake as a risk-factor for diabetic complications and highlights the importance of
48 therapeutic approaches that specifically target the different cell types in DKD.

49 INTRODUCTION

50 Diabetic kidney disease (DKD) is the most common cause of chronic kidney disease
51 (CKD) and end-stage renal failure. It is associated with a large social and economic
52 burden, and there is an unmet need for therapy to halt the progressive course of the
53 disease (6, 37). DKD has been extensively studied during the last decade. Yet there
54 is no uniform concept regarding the cellular mechanisms behind the disease and its
55 progressive course. The majority of studies have focused on the role of one cell type,
56 omitting comparisons. However, given the complexity of the kidney, it is likely that
57 there are several ongoing disease processes, and the development of a therapeutic
58 program that prevents or halts the progressive course of DKD will need to be based
59 on an insight into the ongoing disease processes in each of the target cells in the
60 kidney.

61 The podocytes, proximal tubule cells (PTC) and mesangial cells (MC) are the most
62 commonly studied cells in DKD. Damage and loss of podocytes cause proteinuria
63 and contribute to glomerulosclerosis (23, 47). Damage of tubular cells causes
64 interstitial fibrosis and glomerular tubular dissociation (7, 34). Damage of MC leads to
65 mesangial expansion and contributes to glomerulosclerosis (1, 31). Hyperglycemia
66 and insulin resistance are main causes of diabetic complications (8, 41, 43). Tight
67 glucose control reduces the overall incidence of micro- or macro-albuminuria and
68 halts the progression to end-stage disease (38). Several factors mediate glycemic
69 toxicity, including metabolic dysregulation and generation of advanced glycosylation
70 end products (9). The question whether the adverse effects of glucose
71 concentrations, exceeding the levels in non-diabetic individuals, will also depend on
72 the cellular mechanisms for glucose uptake has often been discussed, but has rarely
73 been addressed experimentally. PTC, which have a high level of aerobic metabolism

74 due to high reabsorption workload (19, 27), takes up glucose via sodium-dependent
75 glucose transporters (SGLT) (24). MC are also reported to express SGLT (20).
76 Podocyte glucose uptake occurs via the insulin sensitive glucose transporter type 4
77 (GLUT4) (14).

78 Glucose related apoptosis was first reported in 1997 by Ortiz and Neilson (36), who
79 showed that immortalized murine renal epithelial cells exposed to 25 mM glucose for
80 at least 24 h caused an upregulation of the apoptotic protein Bax, a downregulation
81 of the anti-apoptotic protein Bcl-xl and triggered apoptosis. Subsequently, most
82 studies of renal apoptosis in DKD have been performed on immortalized renal cells
83 exposed to glucose concentrations that generally by far exceed those commonly
84 observed in the clinical setting. Here we describe the early response of PTC, MC and
85 podocytes when exposed to moderately high (10 and 15 mM) glucose
86 concentrations. All studies were carried out on primary cells, since cell lines undergo
87 mutations, progressively lose their phenotype and have a shift to more anaerobic
88 metabolism. The onset of the mitochondrial apoptotic pathway was used to validate
89 the response to high glucose, since apoptosis marks the transition from reversible to
90 irreversible cell damage and is a common finding in studies of rodent models of DKD
91 (7, 21).

92 **MATERIAL AND METHODS**

93 **Antibodies and Chemicals**

94 The following primary antibodies and dilutions were used: mouse monoclonal anti-
95 Bax [6A7] 5 µg/ml, rabbit polyclonal anti-Bax 1:100, rabbit polyclonal anti-SGLT1
96 1:50, rabbit polyclonal anti-SGLT2 1:100, rabbit polyclonal anti-GLUT4 1:500 and
97 mouse monoclonal anti-alpha smooth muscle actin 1:100 (all from Abcam,

98 Cambridge, UK), rabbit polyclonal anti-SGLT2 1:100 (Fitzgerald Industries
99 International, Acton, MA, USA), rabbit monoclonal anti-Bcl-xl (54H6) 1:200 (Cell
100 Signaling Technology, Inc., Danvers, MA, USA), rabbit polyclonal anti-WT1 1:200
101 (Santa Cruz Biotechnology, Santa Cruz, CA, USA), sheep polyclonal anti-nephrin
102 1:200 (R&D Systems, Inc., Minneapolis, MN, USA) and rabbit polyclonal anti-
103 synaptopodin 1:500 (Sigma-Aldrich, St. Louis, MO, USA). The following fluorescence
104 secondary antibodies were used: Alexa Fluor 488 goat anti-rabbit IgG, Alexa Fluor
105 546 goat anti-mouse IgG and Alexa Fluor 546 goat anti-rabbit IgG (all from Life
106 Technologies, Carlsbad, CA, USA), Star 635P goat anti-rabbit IgG (Abberior,
107 Göttingen, Germany) and Star 635P conjugated to donkey anti-sheep IgG
108 (ThermoFisher Scientific, Waltham, MA, USA) all used in a concentration of 1:500.
109 All antibodies used are commercially available and validated by each manufacturer.
110 All chemicals and reagents were purchased from Sigma-Aldrich, Stockholm,
111 Sweden, and all cell culture and molecular biology materials were purchased from
112 ThermoFisher Scientific, Stockholm, Sweden, unless otherwise stated.

113 **Microscopy**

114 A Zeiss LSM 510 confocal microscope equipped with 25X/0.8NA oil, 40X/1.3NA oil,
115 63X/1.4NA oil and 40X/1.2NA water objectives was used for all imaging of proximal
116 tubule cells (PTC), mesangial cells (MC), primary podocytes and patient material. A
117 Zeiss LSM 780 confocal microscope equipped with 20X/0.8 air and 40X/1.2NA water
118 objectives was used for all imaging of podocyte cell line. Immunofluorescence was
119 detected as follows; CFP with excitation at 405 nm and detection 454-580 nm, DAPI
120 and NucBlue with excitation at 405 nm and detection 420-480 nm, Alexa Fluor 488
121 with excitation at 488 nm and detection 510-550 nm, Alexa Fluor 546 and TUNEL
122 labeling with excitation at 543 nm and 575 nm long pass detection, Star 635P and

123 DRAQ5 with excitation at 633 nm and 650 nm long pass detection. JC-1
124 fluorescence ratios were recorded with excitation at 488 nm and simultaneous 505-
125 530 nm and 560 nm long pass detection. 2-NBDG fluorescence was detected with
126 488 nm excitation and 505 nm long pass detection and DCFDA fluorescence was
127 recorded with 488 nm excitation and 505-550 nm detection.

128 **Animals and Primary cultures**

129 Twenty-day-old male Sprague Dawley rats were used for primary cell preparations.
130 All animals were housed under controlled conditions of light and dark (12:12 h) and
131 given a standard diet containing 20 % protein by weight and tap water were available
132 *ad libitum*. All experiments were performed according to Karolinska Institutet
133 regulations concerning care and use of laboratory animals and were approved by the
134 Stockholm North ethical evaluation board for animal research.

135 Primary culture of rat PTC were prepared as previously described (11). PTC were
136 characterized after 3 days in culture, 99 % of cells were SGLT2-positive (11).

137 Glomeruli isolation and podocyte culture were performed as follows. Rats were
138 anesthetized by intraperitoneal injection of pentobarbital and perfused through the left
139 ventricle with HBSS to clear out blood followed by a solution of HBSS containing
140 Dynabeads M-450. For each animal, 8×10^7 dynabeads in 20 ml of solution was used.
141 After perfusion, kidneys were removed and the medulla was discarded. The cortex
142 was cut to small pieces and digested in 1 mg/ml collagenase I and 10 U/ml DNase in
143 HBSS at 37°C for 30 min with gentle shaking. The digested tissue was gently
144 pressed through a 100- μ m cell strainer (BD Falcon, Bedford, MA, USA). Glomeruli
145 containing dynabeads were collected using a magnetic particle concentrator, washed
146 three times with cold HBSS and seeded on 12 or 18-mm glass coverslips in 12 or 24-
147 well Petri dishes. Podocytes migrated out of glomeruli and were cultured for 3 days in

148 pH 7.4 MEM-NEEA medium supplemented with 3.6 g/l HEPES, 0.5 % insulin-
149 transferrin-selenium-sodium pyruvate, 0.5 % sodium pyruvate, 5 % FBS, 10 µg/ml
150 penicillin and 10 µg/ml streptomycin in 37°C at an approximate humidity of 95–98 %
151 with 5 % CO₂.

152 Primary MC cultures were prepared from isolated glomeruli. The glomeruli were
153 decapsulated by mixing the glomerular suspension with a 1 ml syringe and a 21-
154 gauge needle a couple of times, resuspended in HBSS containing 1 mg/ml
155 collagenase I and digested at 37°C for 15 min with gentle shaking. Cells were
156 resuspended in DMEM supplemented with 2 mM L-glutamine, 20 % FBS, 10 µg/ml
157 penicillin and 10 µg/ml streptomycin and plated in six-well plates. Cells were cultured
158 in 37°C at an approximate humidity of 95–98 % with 5 % CO₂ and culture media was
159 changed every 48 h. After 7 days in culture, each well of cells was split (1:3) in the
160 following way. Cells were washed with Ca²⁺ and Mg²⁺-free PBS pH 7.4 and incubated
161 in 1 ml/well Ca²⁺ and Mg²⁺-free PBS containing 0.05 % trypsin and 0.02 % EDTA for
162 1 min at 37°C. Most of the trypsin solution was removed and cells were incubated for
163 another 3 min. Culture medium containing FBS was added to stop the digestion,
164 wells were split, and new culture medium was added. On the third passage cells
165 were seeded on 12 or 18-mm glass coverslips in 12 or 24-well plates for
166 experiments. Cells were characterized using SGLT1 and alpha smooth muscle actin
167 antibodies, indicating that they were MC.

168 In all experiments using PTC or podocyte cultures, treatment was started on day two
169 or three in culture. MC cultures were used after being passaged three times. Cells
170 were incubated using the following concentrations: 10-30 mM D-glucose and/or 2.5
171 mg/ml delipidated, endotoxin-free albumin (Sigma-Aldrich) with or without 5 nM
172 ouabain (Sigma-Aldrich), 1 µM dapagliflozin (Selleckchem, Munich, Germany) or 0.2

173 mM phlorizin (Selleckchem, Munich, Germany) for 2-24 h as indicated in each figure.
174 As controls, 5.6 mM glucose and mannitol (9.4 mM mannitol + 5.6 mM glucose) was
175 used. Dapagliflozin and phlorizin were dissolved in DMSO, an equal amount DMSO
176 was added to all samples in those experiments as control. Cultures were randomly
177 divided between treatment groups for each experiment.

178 **Immortalized murine podocytes**

179 We use a well described and characterized immortalized mouse podocyte cell line
180 (33). Cells were maintained and differentiated as previously described (26) with the
181 following modifications; culture media was glucose free RPMI 1640 medium
182 supplemented with 5.5 mM D-glucose, 10 % FBS, 10 µg/ml penicillin, 10 µg/ml
183 streptomycin and for undifferentiated cells 10 U/ml interferon gamma (Sigma-
184 Aldrich), cell were differentiated for 7-14 days. The differentiated immortalized
185 podocytes were transiently transfected with SGLT2-ires-CFP (GenScript,
186 Piscataway, NJ, USA) or empty vector CFP (Addgene, Cambridge, MA, USA). The
187 DNA plasmids were delivered to the cells using Lipofectamine LTX reagent with plus
188 reagent (ThermoFisher) diluted in Opti-MEM media (ThermoFisher) according to
189 manufacturer's instructions. Final DNA concentration in each well was 500 ng/ml.
190 Cells were transfected for 48 h and characterized with SGLT2-ires-CFP fluorescence
191 and anti-SGLT2 antibodies.

192 **Immunocytochemical Staining**

193 Following treatment cells were fixed with 4 % paraformaldehyde pH 7.4 and washed
194 three times with PBS. Cells were permeabilized with 0.3 % Triton X-100 for 10 min,
195 washed three times and blocked with 5 % BSA in 0.1 % Triton X-100 for 1 h. Primary
196 antibodies were applied overnight at 4°C. Cells were washed three times and
197 secondary antibodies were applied for 1 h at room temperature. Secondary antibody

198 controls were subjected to the same treatment, but primary antibodies were omitted.
199 The cells were washed three times, mounted with Immu-Mount (Thermo Shandon,
200 Midland, Canada) and imaged with a confocal microscope. In some experiments,
201 cells were counterstained with 1 µg/ml DAPI (Santa Cruz Biotechnology, Inc., USA)
202 for 1-2 min before mounting.

203 **Glucose uptake**

204 Cells were incubated with 100 µM 2-(N-(7-Nitrobenz-2-oxa-1,3-diazol-4-yl)Amino)-2-
205 Deoxyglucose (2-NBDG) (Life Technologies, Carlsbad, USA) in Na⁺ buffer (135 mM
206 NaCl, 5 mM KCl, 1 mM MgSO₄, 0.4 mM K₂HPO₄, 5.5 mM glucose, 20 mM HEPES
207 and 1 mM CaCl₂) or Na⁺-free buffer (NaCl changed for 135 mM choline chloride) pH
208 7.4 for 1 h at 37°C. The last 30 min of incubation, 2 drops/ml NucBlue Live
209 ReadyProbes Reagent (NucBlue) (Life Technologies, Carlsbad, USA) were added to
210 the buffer for nuclear stain. Cells were washed once with Na⁺ or Na⁺-free buffer and
211 imaged with a confocal microscope with fixed settings for all measurements. The
212 glucose uptake was quantified as mean fluorescent intensity of all cells in 5-6
213 separate areas on each coverslip and expressed as:

214 Na⁺-dependent glucose uptake = $(1 - (2\text{-NBDG fluorescence in absence of Na}^+ / 2\text{-NBDG fluorescence in presence of Na}^+)) * 100\%$

216 Average number of cells analyzed from each coverslip was 24 for PTC, 10 for MC
217 and 17 for podocytes.

218 **Detection of apoptotic cells in culture**

219 Cells were fixed in methanol (Solveco AB, Rosersberg, Sweden) for 5 min at 4°C and
220 in ethanol (Solveco AB, Rosersberg, Sweden): acetic acid (2:1) for 5 min at -20°C.
221 After each fixation step the cells were washed with PBS a couple of times. The
222 apoptotic index (AI) was determined with ApopTag Red In Situ Apoptosis Detection

223 kit (TUNEL) (Merk Millipore, Billerica, MA, USA) according to the manufacturer's
224 instructions. The cells were counterstained with 1 µg/ml DAPI for 1-2 min, mounted
225 with Immu-Mount and imaged with a confocal microscope. Cells were considered
226 apoptotic when expressing TUNEL-staining and characteristic apoptotic morphology
227 with condensed nuclei. Total number of cells was determined by DAPI staining and
228 AI was calculated as the percentage of apoptotic cells. For each coverslip 3-5
229 separate areas with at least 100 cells in each image were analyzed except for
230 primary podocytes where approximately 40-50 cells in each image were analyzed. To
231 determine AI of podocytes, podocytes were identified by immunostaining for WT1.
232 Only podocytes outside of a glomerulus and positive for WT1 were included in AI
233 calculations since the total number of podocytes located inside a glomerulus is not
234 possible to determine in this preparation.

235 **SGLT2 knockdown in PTC**

236 SGLT2 gene expression was transiently suppressed using a cocktail of designated
237 siRNAs (Stealth siRNA, cat. no. RSS329982, RSS329983, RSS329984,
238 ThermoFisher). The constructs were delivered into the cells using Lipofectamine
239 RNAiMAX transfection reagent (ThermoFisher) diluted in Opti-MEM media
240 (ThermoFisher) according to manufacturer's instructions. Briefly, the transfection
241 mixture was added to cells culture medium (10 % FBS) at final concentrations of 30
242 nM for each siRNA. Control cells were transfected with 90 nM of a non-targeting
243 construct (Stealth RNAi™ siRNA Negative Control, Med GC, ThermoFisher). Cells
244 were transfected for 48 h before glucose treatment.

245 **Bax, Bcl-xl abundance and translocation assessment**

246 PTC were incubated with mitochondria-targeted green fluorescent protein CellLight
247 Mitochondria-GFP BacMam (Life Technologies, Grand Island, NY, USA) overnight at

248 37°C on day two in vitro and treated with glucose and/or albumin on day three in
249 vitro. MC were incubated with BacMam after being seeded on coverslips for 3-4 days
250 and incubated with glucose the following day. At the end of treatment cells were fixed
251 and immunostained for Bax or Bcl-xl. Microscope setting was kept fixed for all
252 measurements. Bax translocation to the mitochondria was analyzed with Matlab (The
253 MathWorks, Inc., Natick, MA, USA) and calculated as the percentage of overlapping
254 Bax (pixels) with mitochondria (pixels) normalized to cell size (pixels). The total
255 abundance of Bax and Bcl-xl was calculated as the percentage Bax or Bcl-xl (pixels)
256 normalized to cell size (pixels). On each coverslip at least three cells were analyzed.
257 The control group was set to 100 %.

258 **Mitochondrial membrane potential detection**

259 The maintenance of mitochondrial membrane potential ($\Delta\psi_m$) was determined with
260 JC-1 dye (5,5',6,6'-tetrachloro-1,1',3,3'-tetraethylbenzimidazolylcarbocyanid iodine dye)
261 (Lifetime Technologies, Grand Island, NY, USA). JC-1 dye is a cationic carbocyanine
262 dye which accumulates to the mitochondria. At low concentrations the dye is
263 monomeric causing green (527 nm) fluorescence. As the concentration increase, the
264 dye aggregates causing a fluorescence emission shift from green towards red (590
265 nm). A depolarization of the mitochondrial membrane is observed as a decrease in
266 red/green fluorescence ratio. Following glucose treatment cells were washed with
267 Krebs-Ringer pH 7.4 and incubated in culture medium containing 2.5 $\mu\text{g/ml}$ JC-1 for
268 15 min at 37°C. The cells were subjected to live cell imaging using a confocal
269 microscope with fixed settings. The $\Delta\psi_m$ change was quantified as the red (polarized)
270 to green (depolarized) intensity ratio using Matlab. For each coverslip six separate
271 areas were analyzed and all groups were normalized to control.

272 **Reactive oxygen species detection**

273 ROS was measured with Di(Acetoxyethyl Ester) 6-Carboxy-2',7'-
274 Dichlorodihydrofluorescein Diacetate (DCFDA) (ThermoFisher Scientific), where
275 intracellular ROS causes nonfluorescent DCFDA molecules to convert to a green
276 fluorescent form. Following glucose treatment cells were incubated with 10 μ M
277 DCFDA and counterstained with 2 drops/ml of NucBlue for 30 min at 37°C. Cells
278 were rinsed twice with PBS before being subjected to live cell imaging using a
279 confocal microscope with fixed settings for all measurements. ROS was quantified as
280 mean DCFDA intensity in each image. For each coverslip at least 8 individual areas
281 were analyzed. All groups were normalized to control.

282 **Polymerase chain reaction**

283 Cells and tissue samples were collected, and mRNA extracted and purified with
284 RNeasy mini kit (Qiagen, Hilden, Germany) following manufacturer's instructions.
285 PTC were collected as positive control for SGLT2, rat intestine tissue was collected
286 as positive control for SGLT1 and Cos7 were collected as negative control for SGLT1
287 and SGLT2. Reverse transcription was performed using Iscript cDNA synthesis kit
288 (Bio-Rad Laboratories AB, Solna, Sweden) following manufacturer's instructions
289 using 1 μ g sample as starting material. PCR mix was as follows: 1X Phusion GC
290 buffer, 0.2 mM dNTPs, 1.2 mM MgCl₂, 0.5 μ M each for forward and reverse primer, 5
291 % glycerol, 0.02 U/ μ l Phusion polymerase, 2 μ l reverse transcription product for each
292 50 μ l preparation and sterile water. Glycerol was used to prevent aggregation of
293 primers, PCR template and PCR product.

294 Great care was taken to identify specific primers that yielded only one possible PCR
295 product according to Primer Blast. The following primers were used: forward SGLT1
296 *AGTCTACGTAACAGCACAGAAGAGC*, reverse SGLT1 *CTTCCTCCTCTTCCTTAG*

297 *TCATCTT*, forward SGLT2 *CTCTAACATCGCCTACCCACG* and reverse SGLT2
298 *AGAAAGCACCCCTTCTCATTAAACAC*.

299 PCR program was as follows: 98°C for 30 s hot start, 35 cycles: 98°C 10 s, 63°C 15 s
300 and 72°C 30 s, finally 72°C 3 min and 4°C hold.

301 PCR products were separated on agarose gel and visualized using SYBR green I
302 nucleic acid gel stain. The expected PCR product for SGLT1 is 199 bp and for
303 SGLT2 377 bp. The PCR products were purified using GeneJET PCR purification kit
304 following manufacturer's instructions, sequenced (KI-gene, Solna, Sweden) and
305 matched with expected product (Nucleotide Blast) for verification.

306 **Quantitative real-time reverse transcription polymerase chain reaction**

307 Cells were transfected with SGLT2 siRNA (cat. no. RSS329983, Thermo Fisher) or
308 non-targeting construct for 48 h, collected and mRNA were extracted and purified
309 with RNeasy mini kit following manufacturer's instructions. RNA concentration was
310 determined using the Qubit™ RNA HS assay kit and Qubit™ 3.0 fluorometer. The
311 samples were subjected to one-step quantitative real-time reverse transcription
312 polymerase chain reaction measurements using the Quant-X One Step qRT-PCR
313 SYBR Kit (Clontech Laboratories Inc., Mountain View, CA, USA) on a C1000
314 Touch™ Thermal Cycler (Bio-Rad). Each sample was analyzed in duplicates and the
315 SGLT2 expression was analyzed using the $\Delta\Delta C_t$ method described by Pfaffl (39) and
316 GAPDH as house-keeping gene. The following primers were used: Rn_Gapd_1_SG
317 QuantiTect Primer Assay (Qiagen, Hilden, Germany) for GAPDH and forward
318 *CTCTAACATCGCCTACCCACG* and reverse *AGAAAGCACCCCTTCTCATTAAACAC*
319 for SGLT2.

320 **Statistical analysis**

321 All data were expressed as mean \pm SEM. Significance was determined with a one-
322 way ANOVA (single treatment) or a two-way ANOVA (multiple treatments) followed
323 by t-test when applicable. In experiments with only two sample groups a t-test was
324 used. The statistical significance levels are represented as * $p < 0.05$, ** $p < 0.01$ or
325 *** $p < 0.001$ as indicated.

326

327 **RESULTS**

328 Our study is performed on primary cells from rat kidneys. Preparation of cells is
329 described in Figure 1a. PTC and podocytes were studied within 3 days after plating
330 and MC in passage 3, after other glomerular cells had been eliminated. All cells were
331 cultured in a medium containing 5.6 mM glucose prior to the study. Primary PTC
332 culture were prepared from the outer 150 μm of the renal cortex, which has
333 approximately 90 % proximal tubule volume (3) and generates a culture where 99 %
334 of the cells express the SGLT2 isoform during the first three days after plating (11).
335 The late proximal tubular segments express the SGLT1 isoform. MC cells are
336 reported to express either the SGLT1 or the SGLT2 isoform (44, 45). PTC cultured
337 for 3 days stained for SGLT2 and MC stained for SGLT1 (Supplemental Figure S1a,
338 b). A PCR study demonstrated the presence of SGLT1 and 2 mRNA in PTC sample
339 and of SGLT1 mRNA, but not SGLT2 in MC sample (Figure 1b). PCR products were
340 sequenced for verification. To verify that cells express functional SGLT, the basal
341 glucose uptake was determined in all cell types in presence and absence of sodium.
342 Studies were performed in triplicate and repeated three times. Approximately 60 % of
343 PTC glucose uptake and approximately 40 % of MC glucose uptake is sodium
344 dependent. Podocyte glucose uptake is sodium independent. (Figure 1c, d)

345 We first tested the apoptotic effect of short-term exposure to a moderately
346 increased glucose concentration (10-15 mM) in PTC. Cells were TUNEL-stained for
347 determination of apoptotic index (AI). A time and concentration dependent increase
348 in AI was recorded (Figure 2 and Supplemental Figure S2). Since PTC can take up
349 glucose via SGLT as well as GLUT, we questioned whether preventing SGLT-
350 mediated glucose uptake could protect from apoptosis. The apoptotic effect of high
351 glucose exposure to increased extracellular glucose concentration was almost
352 completely abolished in PTC co-incubated with glucose and the SGLT2 inhibitor
353 dapagliflozin compared to glucose alone (Figure 3a). To further validate the role of
354 SGLT2 in glucose triggered apoptosis, we downregulated the SGLT2 expression in
355 PTC with siRNA for 48 h. The siRNA treatment reduced SGLT2 mRNA levels (Figure
356 3c) and prevented glucose induced apoptosis (Figure 3b). The level of AI in control
357 cells with SGLT2 siRNA and negative control was comparable. The possibility that
358 increased osmotic pressure was responsible for the apoptotic effect was excluded by
359 parallel studies using mannitol instead of glucose (Supplemental Table S1). Since
360 few studies have documented the relevance of apoptosis in human DKD, we re-
361 examined biopsy specimens from five male patients with DKD with regard to
362 apoptosis and compared them with biopsies from three male healthy kidney donors
363 in corresponding age (Supplemental Figure S3b). The number of tubules with
364 apoptotic cells in DKD patients was 3 fold higher than in control individuals
365 (Supplemental Figure S3a, c). An aggregation of apoptotic cells in cross-sections of
366 tubular lumen was often observed in the biopsies from DKD patients (Supplemental
367 Figure S3d).

368 Several lines of evidence suggest that hyperglycemic toxicity is associated with
369 activation of the mitochondrial apoptotic pathway, controlled by the Bcl family of

370 proteins to which the apoptotic protein Bax and the anti-apoptotic protein Bcl-xl
371 belong (12, 16). Under healthy condition, Bcl-xl mainly resides on the mitochondria,
372 whereas Bax is located both in cytosol and on mitochondria. During the course of
373 apoptosis, the abundance of Bcl-xl decreases and the abundance of Bax increases
374 allowing Bax to translocate from cytosol to mitochondria, where it will ultimately
375 permeabilize the mitochondrial membrane, which marks the point of no return in the
376 apoptotic process (Figure 4a). Figure 4b and c show PTC immune-stained for Bcl-xl
377 and Bax, respectively. Mitochondria are visualized with mitochondrial targeted GFP.
378 Quantification of the fluorescent signals show decreased expression of Bcl-xl and
379 increased expression and mitochondrial location of Bax in PTC after 4-8 h exposure
380 to 15 mM glucose (Figure 4d-f). The ongoing apoptotic process was accompanied by
381 a decrease in mitochondrial membrane potential and an increase of reactive oxygen
382 species (Figure 4g, h and Supplemental Figure S4).

383 Proteinuria is a hallmark of DKD. Since proteinuric kidney disease is known to be
384 associated with PTC apoptosis (11), we next examined if co-exposure to threshold
385 concentrations of glucose and albumin would have an additive effect. Cells were
386 exposed to glucose (10 mM) and albumin (2.5 mg/ml) either alone or in combination
387 for 8 h (Figure 5a). Albumin concentration was selected based on our previous study
388 (11), where we show that albumin triggers apoptosis in a dose-dependent manner in
389 PTC. Cells co-exposed to glucose and albumin had significantly higher AI than cells
390 exposed to glucose or albumin alone (Figure 5b). Cells co-exposed to glucose and
391 albumin, in contrast to cells exposed to either substance alone, had a significant
392 increase in Bax abundance and Bax translocation to the mitochondria compared to
393 control (Figure 5c, d).

394 MC also exhibited high sensitivity to short-term high glucose exposure. A significant
395 increase in AI was recorded in cells exposed to 15 mM glucose for 8 h (Figure 6a).
396 Activation of the mitochondrial apoptotic pathway was confirmed by decreased Bcl-xl
397 abundance, increased Bax abundance and translocation of Bax to the mitochondria
398 (Figure 6b-f). No apoptotic response was observed in MC exposed to 15 mM glucose
399 and co-incubated with phlorizin, a non-selective inhibitor of SGLT 1 and 2 (Figure
400 6g).

401 We have previously shown that sub-saturating concentrations of ouabain activates a
402 Na,K-ATPase/IP3 receptor signaling pathway (2) and that down-stream effects
403 involve protection from apoptosis in rat PTC exposed to excessive concentrations of
404 albumin (11) and Shiga toxin (10). Here we show that ouabain 5 nM, which has no
405 effect on intracellular sodium concentration (28), also protects from glucose-triggered
406 apoptosis in SGLT expressing cells (Table 1 and 2). Ouabain 5 nM rescued from
407 apoptosis and changes in Bax and Bcl-xl expression in PTC and MC exposed to 15
408 mM glucose for 8 h, and in PTC co-exposed to glucose and albumin for 8 h. Ouabain
409 5 nM also protected from mitochondrial depolarization and increased ROS formation
410 in PTC exposed to 15 mM glucose for 4 and 8 h.

411 The podocytes were cultured for 3 days and did at that time express the podocyte
412 specific proteins; nephrin, synaptopodin and WT1 (Figure 7a) as well as GLUT4
413 (Supplemental Figure S1c). The culture medium contained 0.85 μ M insulin. The
414 podocytes were first exposed to 15 mM glucose for 8 h. Surprisingly, we found no
415 increase in AI (Figure 7b, f). Nor was there any increase in ROS (Figure 7c). The AI
416 for podocytes was, under control conditions, in the same range as the AI for proximal
417 tubular and mesangial cells studied under control conditions (Supplemental Table

418 S1). In the majority of previous studies on the response of immortalized podocytes to
419 high glucose exposure, the glucose concentration has been around 25 mM or higher
420 (25, 29, 42). Therefore, we next tested whether 8 or 24 h exposure to 30 mM glucose
421 would provoke apoptosis in podocytes. This was not the case (Figure 7d-f).
422 Immortalized podocytes transfected with SGLT2 vector expressed the protein (Figure
423 8a, b), but did not display sodium-dependent glucose uptake (Figure 8c, d) and did
424 not respond with apoptosis following exposure to 15 mM glucose for 8 h (Figure 8e).

425 **DISCUSSION**

426 This is the first ex vivo study comparing the early response to a moderate increase in
427 glucose concentrations in three DKD target cells. Our study highlights the importance
428 of using primary cells for understanding the disease process and provides
429 experimental evidence for the hypothesis that cells that are less efficient in adapting
430 their glucose uptake are particularly vulnerable to the acute effects of hyperglycemia.

431 The majority of our studies were performed on PTC, which mainly express the high
432 capacity, low affinity SGLT2 isoform. Even modest increases in extracellular glucose
433 evoked an SGLT dependent prompt apoptotic response in a small but significant
434 fraction of PTC and MC. The apoptotic response is directly related to excessive
435 glucose uptake via the SGLT transporters, since apoptosis was not observed
436 following inhibition or down-regulation of SGLT. The SGLT glucose uptake is
437 energized by the sodium gradient generated by Na,K-ATPase transporting 3 Na⁺ out
438 of the cell and 2 K⁺ into the cell, at the cost of 1 ATP. We showed several years ago
439 that exposure of rat proximal tubules to high glucose concentrations results in
440 increased Na,K-ATPase activity and Na,K-ATPase dependent energy consumption
441 (27) (Supplemental Figure S5). This implies that sodium-dependent glucose transport

442 via SGLT lacks a robust negative feedback control to protect against excessive
443 glucose uptake. Primary podocytes had no measurable sodium-dependent glucose
444 uptake and were resistant to the short-term apoptotic effects of high glucose
445 exposure. Podocytes express GLUT4, which is located in intracellular vesicles that
446 are translocated to the plasma membrane in an insulin-dependent manner. The
447 insulin-signaling pathway has a well-developed negative feedback control via the
448 state of activity of several signaling proteins, including the Rab-GTPase-activating.
449 Podocytes transfected with SGLT2 vector did not exhibit a sodium-dependent
450 glucose uptake and did not respond to high glucose exposure with apoptosis,
451 suggesting a more complex relationship between SGLT and Na,K-ATPase than what
452 was previously believed.

453 The high sensitivity of PTC to moderately increased extracellular glucose
454 concentrations raises the question whether PTC are targeted already at the onset of
455 diabetes. DKD is rarely diagnosed during the early phase of diabetes, but it is
456 conceivable that DKD exists for a long time as an incipient disease, since the kidney
457 has a high reserve capacity and renal epithelial cells have a relatively high
458 regenerative capacity (17). Albuminuria is both a biomarker and a risk factor in CKD,
459 and excessive albumin uptake in renal epithelial cells is accompanied by a time- and
460 dose-dependent activation of the mitochondrial apoptotic pathway (11). Exposure of
461 PTC to both albumin and glucose resulted in more extensive apoptosis than
462 exposure to albumin or glucose alone. This finding may offer an explanation to the
463 common clinical observation that onset of micro-albuminuria is associated with
464 accelerated decay of renal function (22). Since apoptosis is accompanied by
465 increased secretion of TGF-beta and other pro-inflammatory products that drive a
466 fibrotic process (32, 40), we propose that acute apoptotic responses of PTC to

467 repeated episodes of hyperglycemia is a major cause of the progressive interstitial
468 fibrosis in DKD. Podocytes do not regenerate and are generally considered the weak
469 link in DKD (30, 41). Our study suggests that hyperglycemia does not exert an
470 immediate toxic effect on the podocytes, and that other factors, such as exposure to
471 glycated proteins and lack and/or resistance to insulin are more likely to be the
472 primary cause of podocyte injury (13, 41).

473 Ouabain has been demonstrated to rescue PTC from apoptosis in animal models of
474 proteinuric disease (11) and hemolytic uremic syndrome (10) when given in sub-
475 saturating non-toxic concentrations. Here we showed that ouabain 5 nM rescued
476 both PTC and MC from the onset of high glucose triggered apoptosis. These findings
477 have implications for the future design of a therapy that aims to halt the progressive
478 course of DKD by preventing apoptosis.

479 SGLT2 inhibitors are widely used as blood glucose lowering agents in diabetic
480 treatment (46, 49). Their protective effect with regard to cardiovascular outcome is
481 well documented, while the effect on DKD is still being evaluated (15, 35, 48, 50).
482 Since SGLT2 inhibitors should increase the glucose load to the SGLT1 expressing
483 late PTC, the overall reno-protective effect is difficult to predict and need further
484 studies. Our study points to a previously unappreciated role of SGLT transporters for
485 diabetic complications. The vulnerability of SGLT 1 and 2 expressing cells to short-
486 term exposure to increased extracellular glucose concentrations should have
487 implications for many SGLT expressing cell types, including cardiomyocytes,
488 endothelial cells and pancreatic alpha islet cells (4, 5, 18). Currently there is little
489 information available about the acute response of these cells to high glucose
490 exposure.

491 **ACKNOWLEDGMENTS**

492 We are grateful to the patients and those who carried out the work in relation to the
493 biopsies at Department of Renal Medicine, Karolinska University Hospital and The
494 Karolinska Kidney Research Center – KaroKidney. The authors thank Minttu Virkki
495 and Evgeny Akkuratov for experimental assistance.

496 **GRANTS**

497 This study was supported by the Swedish Research Council to A.A and H.B, the
498 Erling-Persson Family Foundation and Torsten Söderberg Foundation to A.A,
499 Märta and Gunnar V. Philipsons Foundation and Magnus Bergvalls Foundation to
500 L.S. D.S. is supported by a Novo Nordisk postdoctoral fellowship run in partnership
501 with Karolinska Institutet.

502

- 504 1. **Abrass CK.** Diabetic nephropathy. Mechanisms of mesangial matrix
505 expansion. *West J Med* 162: 318-321, 1995.
- 506 2. **Aperia A, Akkuratov EE, Fontana JM, Brismar H.** Na⁺-K⁺-ATPase, a new
507 class of plasma membrane receptors. *Am J Physiol Cell Physiol* 310: C491-
508 C495, 2016.
- 509 3. **Aperia A, Larsson L, Zetterström R.** Hormonal induction of Na-K-ATPase in
510 developing proximal tubular cells. *Am J Physiol* 241: F356-F360, 1981.
- 511 4. **Banerjee SK, McGaffin KR, Pastor-Soler NM, Ahmad F.** SGLT1 is a novel
512 cardiac glucose transporter that is perturbed in disease states. *Cardiovasc*
513 *Res* 84: 111-118, 2009.
- 514 5. **Bonner C, Kerr-Conte J, Gmyr V, Queniat G, Moerman E, Thévenet J,**
515 **Beaucamps C, Delalleau N, Popescu I, Malaisse WJ, Sener A, Deprez, B,**
516 **Abderrahmani A, Staels B, Pattou F.** Inhibition of the glucose transporter
517 SGLT2 with dapagliflozin pancreatic alpha cells triggers glucagon secretion.
518 *Nat Med* 21: 512-517, 2015.
- 519 6. **Breyer M, Susztak K.** The next generation of therapeutics for chronic kidney
520 disease. *Nat Rev Drug Discov* 15: 568-588, 2016.
- 521 7. **Brezniceanu ML, Liu F, Wei CC, Chénier I, Godin N, Zhang SL, Filep JG,**
522 **Ingelfinger JR, Chan JS.** Attenuation of interstitial fibrosis and tubular
523 apoptosis in db/db transgenic mice overexpressing catalase in renal proximal
524 tubular cells. *Diabetes* 57: 451-459, 2008.
- 525 8. **Brownlee M.** Biochemistry and molecular cell biology of diabetic
526 complications. *Nature* 414: 813-820, 2001.
- 527 9. **Brownlee M.** Glycation products and the pathogenesis of diabetes
528 complications. *Diabetes Care* 15: 1835-1843, 1992.
- 529 10. **Burlaka I, Liu XL, Rebetz J, Arvidsson I, Yang L, Brismar H, Karpman D,**
530 **Aperia A.** Ouabain protects from Shiga toxin-triggered apoptosis by reversing
531 the imbalance between Bax and Bcl-xL. *J Am Soc Nephrol* 24: 1413-1423,
532 2013.
- 533 11. **Burlaka I, Nilsson LM, Scott L, Holtbäck U, Eklöf AC, Fogo AB, Brismar**
534 **H, Aperia A.** Prevention of apoptosis averts glomerular tubular disconnection
535 and podocyte loss in proteinuric kidney disease. *Kidney Int* 90: 135-148, 2016.
- 536 12. **Chen HC, Kanai M, Inoue-Yamauchi A, Tu HC, Huang Y, Ren D, Kim H,**
537 **Takeda S, Reyna DE, Chan PM, Ganesan YT, Liao CP, Gavathiotis E,**
538 **Hsieh JJ, Cheng EH.** An interconnected hierarchical model of cell death
539 regulation by the BCL-2 family. *Nat Cell Biol* 17: 1270-128, 2015.
- 540 13. **Coward R, Fornoni A.** Insulin signaling: implications for podocyte biology in
541 diabetic kidney disease. *Curr Opin Nephrol Hypertens* 24: 104–110, 2015.
- 542 14. **Coward RJ, Welsh GI, Yang J, Tasman C, Lennon R, Koziell A, Satchell**
543 **S, Holman GD, Keriaschki D, Tavaré JM, Mathieson PW, Saleem MA.** The
544 human glomerular podocyte is a novel target for insulin action. *Diabetes* 54:
545 3095-3102, 2015.
- 546 15. **DeFronzo RA, Norton L, Abdul-Ghani M.** Renal, metabolic and
547 cardiovascular considerations of SGLT2 inhibition. *Nat Rev Nephrol* 13: 11-26,
548 2017.
- 549 16. **Edlich F, Banerjee S, Suzuki M, Cleland MM, Arnoult D, Wang C,**
550 **Neutzner A, Tiandra N, Youle RJ.** Bcl-xL retrotranslocates Bax from the
551 mitochondria into the cytosol. *Cell* 145: 104-116, 2011.

- 552 17. **Gilbert RE.** Proximal tubulopathy: prime mover and key therapeutic target in
553 diabetic kidney disease. *Diabetes* 66: 791-800, 2017.
- 554 18. **Han Y, Cho YE, Ayon R, Guo R, Youssef KD, Pan M, Dai A, Yuan JX,**
555 **Makino A.** SGLT inhibitors attenuate NO-dependent vascular relaxation in the
556 pulmonary artery but not in the coronary artery. *Am J Physiol Lung Cell Mol*
557 *Physiol* 309: L1027-L1036, 2015.
- 558 19. **Hansell P, Welch WJ, Blantz RC, Palm F.** Determinants of kidney oxygen
559 consumption and their relationship to tissue oxygen tension in diabetes and
560 hypertension. *Clin Exp Pharmacol Physiol* 40: 123-137, 2013.
- 561 20. **Heilig CW, Brosius FC 3rd, Henry DN.** Glucose transporters of the
562 glomerulus and the implications for diabetic nephropathy. *Kidney Int Suppl* 60:
563 S91-S99, 1997.
- 564 21. **Hou Y, Li S, Wu M, Wei J, Ren Y, Du C, Wu H, Han C, Duan H, Shi Y.**
565 Mitochondria-targeted peptide SS-31 attenuates renal injury via an antioxidant
566 effect in diabetic nephropathy. *Am J Physiol Renal Physiol* 310: F547-F559,
567 2016.
- 568 22. **Huang S, Czech MP.** The GLUT4 glucose transporter. *Cell Metab* 5: 237-252,
569 2007.
- 570 23. **Inoki K, Mori H, Wang J, Suzuki T, Hong S, Yoshida S, Blattner SM,**
571 **Ikenoue T, Rüegg MA, Hall MN, Kwiatkowski DJ, Rastaldi MP, Huber TB,**
572 **Kretzler M, Holzman LB, Wiggins RC, Guan KL.** mTORC1 activation in
573 podocytes is a critical step in the development of diabetic nephropathy in
574 mice. *J Clin Invest* 121: 2181-2196, 2011.
- 575 24. **Kanai Y, Lee WS, You G, Brown D, Hediger MA.** The human kidney low
576 affinity Na⁺/glucose cotransporter SGLT2. Delineation of the major renal
577 reabsorptive mechanism for D-glucose. *J Clin Invest* 93: 397-404, 1994.
- 578 25. **Khazim K, Gorin Y, Cavaglieri RC, Abboud HE, Fanti P.** The antioxidant
579 silybin prevents high glucose-induced oxidative stress and podocyte injury in
580 vitro and in vivo. *Am J Physiol Renal Physiol* 305: F691-F700, 2013.
- 581 26. **Kim EY, Choi KJ, Dryer SE.** Nephrin binds to the COOH terminus of a large-
582 conductance Ca²⁺-activated K⁺ channel isoform and regulates its expression
583 on the cell surface. *Am J Physiol Renal Physiol* 295: F235-F246, 2008.
- 584 27. **Körner A, Eklöf AC, Celsi G, Anita A.** Increased renal metabolism in
585 diabetes. Mechanism and functional implications. *Diabetes* 43: 629-633, 1994.
- 586 28. **Li J, Khodus GR, Kruusmägi M, Kamali-Zare P, Liu XL, Eklöf AC, Zelenin**
587 **S, Brismar H, Aperia A.** Ouabain protects against adverse developmental
588 programming of the kidney. *Nat Commun* 1: 42, 2010.
- 589 29. **Li W, Wang Q, Du M, Ma X, Wu L, Guo F, Zhao S, Huang F, Wang H, Qin**
590 **G.** Effects of overexpressing FoxO1 on apoptosis in glomeruli of diabetic mice
591 and in podocytes cultured in high glucose medium. *Biochem Biophys Res*
592 *Commun* 478: 612-617, 2016.
- 593 30. **Lin JS, Susztak K.** Podocytes: the weakest link in diabetic kidney disease?
594 *Curr Diab Rep* 16: 45, 2016.
- 595 31. **Mason RM, Wahab NA.** Extracellular matrix metabolism in diabetic
596 nephropathy. *J Am Soc Nephrol* 14: 1358-1373, 2003.
- 597 32. **Meng XM, Nikolic-Paterson DJ, Lan HY.** TGF- β : the master regulator of
598 fibrosis. *Nat Rev Nephrol* 12: 325-338, 2016.
- 599 33. **Mundel P, Reiser J, Zúñiga Mejía Borja A, Pavenstädt H, Davidson GR,**
600 **Kriz W, Zeller R.** Rearrangements of the cytoskeleton and cell contacts

- 601 induce process formation during differentiation of conditionally immortalized
602 mouse podocyte cell lines. *Exp Cell Res* 236: 248–58, 1997.
- 603 34. **Najafian B, Kim Y, Crosson JT, Mauer M.** Atubular glomeruli and
604 glomerulotubular junction abnormalities in diabetic nephropathy. *J Am Soc*
605 *Nephrol* 14: 908-917, 2003.
- 606 35. **Novikov A, Vallon V.** Sodium glucose cotransporter 2 inhibition in the diabetic
607 kidney: an update. *Curr Opin Nephrol Hypertens* 25: 50-58, 2016.
- 608 36. **Ortiz A, Ziyadeh FN, Neilson EG.** Expression of apoptosis-regulatory genes
609 in renal proximal tubular epithelial cells exposed to ambient glucose and in
610 diabetic kidneys. *J Investig Med* 45: 50-56, 1997.
- 611 37. **Ozieh MN, Dismuke CE, Lynch CP, Egede LE.** Medical care expenditures
612 associated with chronic kidney disease in adults with diabetes: United States
613 2011. *Diabetes Res Clin Pract* 109: 185-190, 2015.
- 614 38. **Perkovic V, Heerspink HL, Chalmers J, Woodward M, Jun M, Li Q,**
615 **MacMahon S, Cooper ME, Hamet P, Marre M, Mogensen CE, Poulter N,**
616 **Mancia G, Cass A, Patel A, Zoungas S, ADVANCE Collaborative Group.**
617 Intensive glucose control improves kidney outcomes in patients with type 2
618 diabetes. *Kidney Int* 83: 517-523, 2013.
- 619 39. **Pfaffl MW.** A new mathematical model for relative quantification in real-time
620 RT-PCR. *Nucleic acids research* 29: e45, 2001.
- 621 40. **Ramesh S, Wildey GM, Howe PH.** Transforming growth factor β (TGF β)-
622 induced apoptosis. *Cell Cycle* 8: 11-17, 2009.
- 623 41. **Reidy K, Kang HM, Hostetter T, Susztak K.** Molecular mechanisms of
624 diabetic kidney disease. *J Clin Invest* 134: 2333-2340, 2014.
- 625 42. **Susztak K, Raff AC, Schiffer M, Böttinger EP.** Glucose-induced reactive
626 oxygen species cause apoptosis of podocytes and podocyte depletion at the
627 onset of diabetic nephropathy. *Diabetes* 55: 225-233, 2006.
- 628 43. **Thomas MC, Brownlee M, Susztak K, Sharma K, Jandeleit-Dahm KA,**
629 **Zoungas S, Rossing P, Groop PH, Cooper ME.** Diabetic kidney disease.
630 *Nat Rev Dis Primers* 1:15018, 2015.
- 631 44. **Wakisaka M, He Q, Spiro MJ, Spiro RG.** Glucose entry into rat mesangial
632 cells is mediated by both Na(+)-coupled and facilitative transporters.
633 *Diabetologia* 38: 291-297, 1995.
- 634 45. **Wakisaka M, Nagao T, Yoshinari M.** Sodium glucose cotransporter 2
635 (SGLT2) plays as a physiological sensor and regulates cellular contractility in
636 rat mesangial cells. *PLoS One* 11: e0151585, 2016.
- 637 46. **Weber MA, Mansfield TA, Cain VA, Iqbal N, Parikh S, Ptaszynska A.** Blood
638 pressure and glycaemic effects of dapagliflozin versus placebo in patients with
639 type 2 diabetes on combination antihypertensive therapy: a randomised,
640 double-blind, placebo-controlled, phase 3 study. *Lancet Diabetes Endocrinol*
641 4: 211-220, 2016.
- 642 47. **Weil EJ, Lemley KV, Mason CC, Yee B, Jones LI, Blouch K, Lovato T,**
643 **Richardson M, Myers BD, Nelson RG.** Podocyte detachment and reduced
644 glomerular capillary endothelial fenestration promote kidney disease in type 2
645 diabetic nephropathy. *Kidney Int* 82: 1010-1017, 2012.
- 646 48. **Wu JH, Foote C, Blomster J, Toyama T, Perkovic V, Sundström J, Neal B.**
647 Effects of sodium-glucose cotransporter-2 inhibitors on cardiovascular events,
648 death, and major safety outcomes in adults with type 2 diabetes: a systematic
649 review and meta-analysis. *Lancet Diabetes Endocrinol* 4: 411-419, 2016.

- 650 49. Yamout H, Perkovic V, Davies M, Woo V, de Zeeuw D, Mayer C,
651 Viiapurkar U, Kline I, Usiskin K, Meininger G, Bakris G. Efficacy and safety
652 of canagliflozin in patients with type 2 diabetes and stages 3 nephropathy. *Am*
653 *J Nephrol* 40: 64-74, 2014.
- 654 50. Zinman B, Wanner C, Lachin JM, Fitchett D, Bluhmki E, Hantel S,
655 Mattheus M, Devins T, Johansen OE, Woerle HJ, Broedl UC, Inzucchi SE;
656 **EMPA-REG OUTCOME Investigators**. Empagliflozin, cardiovascular
657 outcomes, and mortality in type 2 diabetes. *N Engl J Med* 373: 2117-2128,
658 2015.

Variable	Cell type	Control	Glucose	Glucose Ouabain	n (#prep)
AI (%)	PTC	3.1 ± 0.1	7.5 ± 0.3	2.9 ± 0.2	9 (3)
Bcl-xl expression (%)	PTC	100	68 ± 4	97 ± 7	15 (5)
Bax expression (%)	PTC	100	155 ± 14	124 ± 9	15 (5)
Bax/mito overlap (%)	PTC	100	144 ± 14	118 ± 9	15 (5)
$\Delta\psi_m$ (%)	PTC	100	66 ± 6	89 ± 5	3 (3)
ROS (%)	PTC	100	143 ± 9	118 ± 11	8 (2)
AI (%)	MC	3.1 ± 0.3	5.3 ± 0.7	3.3 ± 0.5	12 (4)
Bcl-xl expression (%)	MC	100	62 ± 3	97 ± 6	12 (4)
Bax expression (%)	MC	100	162 ± 19	118 ± 19	13 (5)
Bax/mito overlap (%)	MC	100	153 ± 24	96 ± 14	13 (5)

659

660 **Table 1. Ouabain rescues PTC and MC from high-glucose induced apoptosis**

661 Quantification of AI, Bcl-xl abundance, Bax abundance and accumulation on
662 mitochondria, mitochondrial membrane potential ($\Delta\psi_m$) and ROS in PTC and MC
663 incubated with control (5.6 mM), 15 mM glucose or 15 mM glucose + 5 nM ouabain
664 containing medium for 8 h as indicated. Table shows mean ± SEM. n = number of
665 coverslips, #prep = number of cell preparations.

666

Variable	Cell type	Control	Glucose Albumin	Glucose Albumin Ouabain
AI (%)	PTC	3.0 ± 0.2	7.4 ± 0.4	3.4 ± 0.4
Bax expression (%)	PTC	100	149 ± 12	104 ± 8
Bax/mito overlap (%)	PTC	100	170 ± 22	124 ± 16

667 **Table 2. Ouabain rescues PTC from high glucose and albumin induced**
668 **apoptosis** Quantification of AI, Bax abundance and accumulation on mitochondria in
669 PTC incubated with control (5.6 mM), 15 mM glucose + 2.5 mg/ml albumin or 15 mM
670 glucose + 2.5 mg/ml albumin + 5 nM ouabain containing medium for 8 h as indicated.
671 Table shows mean ± SEM. n = 9 coverslips from 3 individual cell preparations.

672 **LEGENDS**

673 **Figure 1. Cell preparation; Documentation of SGLT expression in PTC and MC**

674 (a) PTC (left) were prepared by digesting the outer cortex (150 μm) of rat kidneys into
675 single cells, allowing the cells to culture for 2-3 days before characterizing the cells
676 with SGLT2 antibodies. MC (middle) were prepared by perfusing rats with magnetic
677 beads, extracting glomeruli containing beads with a magnetic collector and digesting
678 the glomeruli to single cells. Following, passage 3 MC were characterized with alpha-
679 smooth muscle actin (α -SMA) antibodies. Podocytes (right) were prepared from
680 extracted glomeruli as for MC. Glomeruli were plated for 3 days letting the podocytes
681 move out from the glomerulus. Podocytes were characterized with WT1 antibodies.
682 (b) PCR for SGLT1 (left) and SGLT2 (right) in PTC, MC, Cos7 and intestine tissue as
683 indicated. Arrows show 199 bp for SGLT1 and 377 bp for SGLT2. (c) Glucose uptake
684 in PTC (left), MC (middle) and podocytes (right) measured with 2-NBDG (green) in
685 Na^+ (upper panel) or Na^+ -free (lower panel) buffer (5.6 mM glucose). Cells were
686 counterstained with NucBlue (blue). Scale bars 20 μm . (d) Quantification of Na^+ -
687 dependent glucose uptake in PTC, MC and podocytes. Data are expressed as mean
688 \pm SEM. n=9 coverslips for PTC and n=8 coverslips for MC from 3 individual cell
689 preparations. n=5 coverslips from 2 individual cell preparations for podocytes.
690 *p<0.05, ***p<0.001

691 **Figure 2. Short-time apoptotic response of PTC to increased glucose**

692 **concentration** (a) PTC stained with TUNEL (red) and DAPI (blue). PTC were
693 incubated with control (5.6 mM) or 15 mM glucose containing medium for 2, 4 and 8
694 h. Scale bars 40 μm . (b, c) Quantification of AI in PTC incubated with control, 10 mM
695 glucose in (b) or 15 mM glucose in (c) containing medium for 2, 4 and 8 h.
696 Approximately 100-200 cells in 5 separate areas of each coverslip were counted.

697 Data are expressed as mean \pm SEM. n=9 coverslips from 3 individual cell
698 preparations. *p<0.05, ***p<0.001

699 **Figure 3. SGLT2 inhibition with dapagliflozin or knockdown with siRNA**
700 **protects from high glucose induced apoptosis in PTC** (a) Quantification of AI in
701 PTC incubated with control (5.6 mM), 15 mM glucose or 15 mM glucose + 1 μ M
702 dapagliflozin containing medium for 8 h. Dapagliflozin was dissolved in DMSO, an
703 equal amount DMSO was added to all samples as control. Data are expressed as
704 mean \pm SEM. n=9 coverslips from 3 individual cell preparations. (b) Top panel: Time-
705 line for siRNA silencing. Bottom panel: Quantification of AI in PTC transfected with
706 SGLT2 or negative control (nc) siRNA for 48 h and incubated with control or 15 mM
707 glucose for 8 h. Data are expressed as mean \pm SEM. n=6 coverslips from 2 individual
708 cell preparations. (c) Quantification of SGLT2 mRNA expression following siRNA
709 exposure for 48 h. Data are expressed as mean \pm SEM. n=3 cell preparations.
710 **p<0.01, ***p<0.001

711 **Figure 4. High glucose triggers apoptosis via the mitochondrial pathway in a**
712 **time-dependent manner in PTC** (a) Cartoon illustrating activation of the
713 mitochondrial apoptotic pathway. In normal condition, there is a balance between
714 Bcl-xl and Bax preventing apoptosis. When an apoptotic stimulus, i.e. high glucose,
715 activates the intrinsic apoptotic pathway, the balance between Bax and Bcl-xl is
716 disrupted which leads to mitochondrial dysfunction (decreased $\Delta\psi_m$) and apoptosis.
717 (b, c) Immunofluorescence staining for Bcl-xl (b) and Bax (c) expression (red) in PTC
718 incubated with control (5.6 mM) or 15 mM glucose containing medium for 8 h.
719 Mitochondria are shown in green. Scale bars 10 μ m. (d-f) Quantification of Bcl-xl
720 abundance (d), Bax abundance (e) and Bax accumulation on mitochondria (f) in PTC
721 incubated with control or 15 mM glucose containing medium for 2, 4 and 8 h. Data

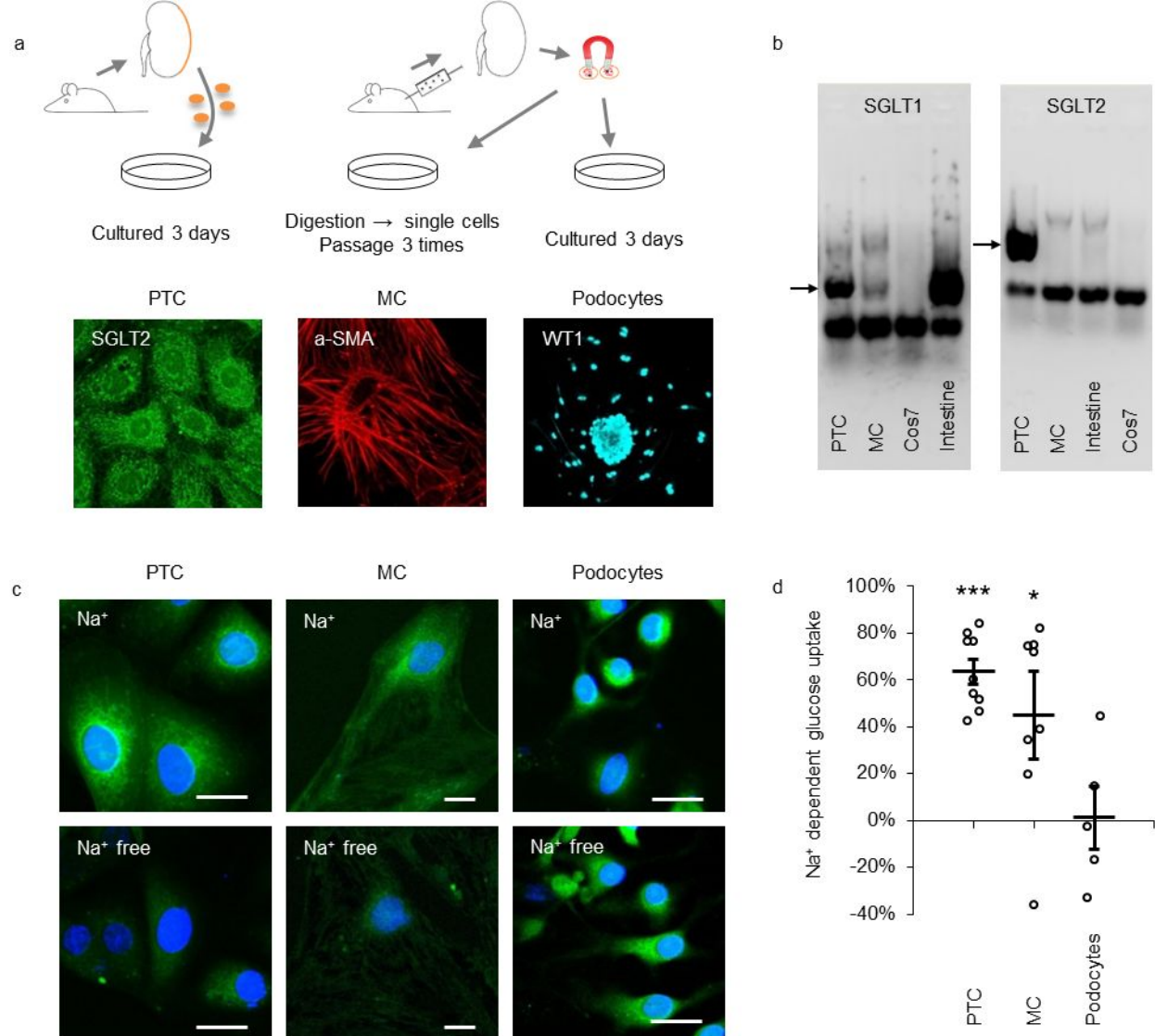
722 are expressed as mean \pm SEM. n=15 coverslips from 5 individual cell preparations.
723 (g) Quantification of $\Delta\psi_m$ in PTC incubated with control or 15 mM glucose containing
724 medium for 2, 4 and 8 h. Data are expressed as mean \pm SEM. n=3 coverslips from 3
725 individual cell preparations. (h) Quantification of ROS in PTC incubated with control
726 or 15 mM glucose containing medium for 4 h. Data are expressed as mean \pm SEM.
727 n=8 coverslips from 2 individual cell preparations. *p<0.05, **p<0.01 ***p<0.001

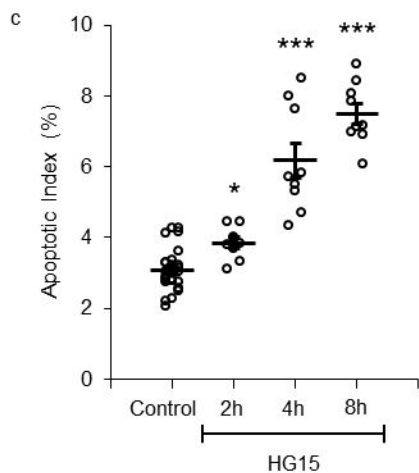
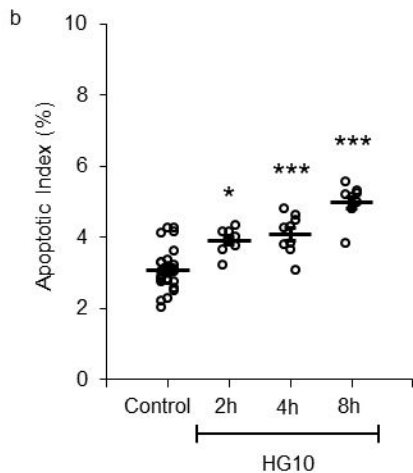
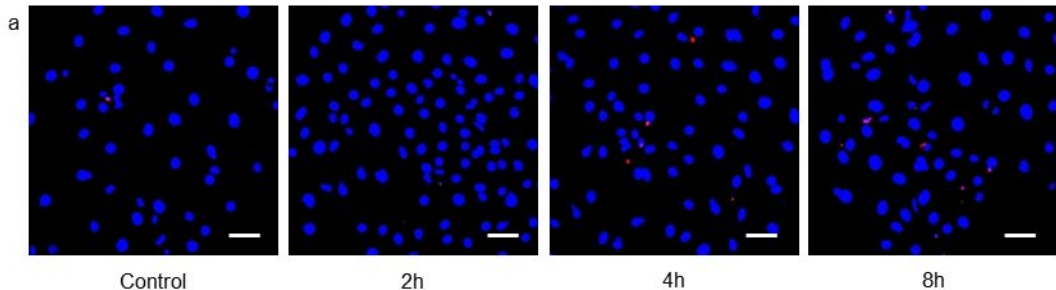
728 **Figure 5. Short-time apoptotic response of PTC co-incubated with high glucose**
729 **and albumin** (a) Cartoon illustrating uptake of high glucose (red arrow) and albumin
730 (purple arrow) in PTC. (b-d) Quantification of AI (b), Bax abundance (c) and Bax
731 accumulation on mitochondria (d) in PTC incubated with control (5.6 mM), 10 mM
732 glucose, 2.5 mg/ml albumin or 10 mM glucose + 2.5 mg/ml albumin containing
733 medium for 8 h. Data are expressed as mean \pm SEM. n=9 coverslips from 3
734 individual cell preparations. *p<0.05, **p<0.01, ***p<0.001

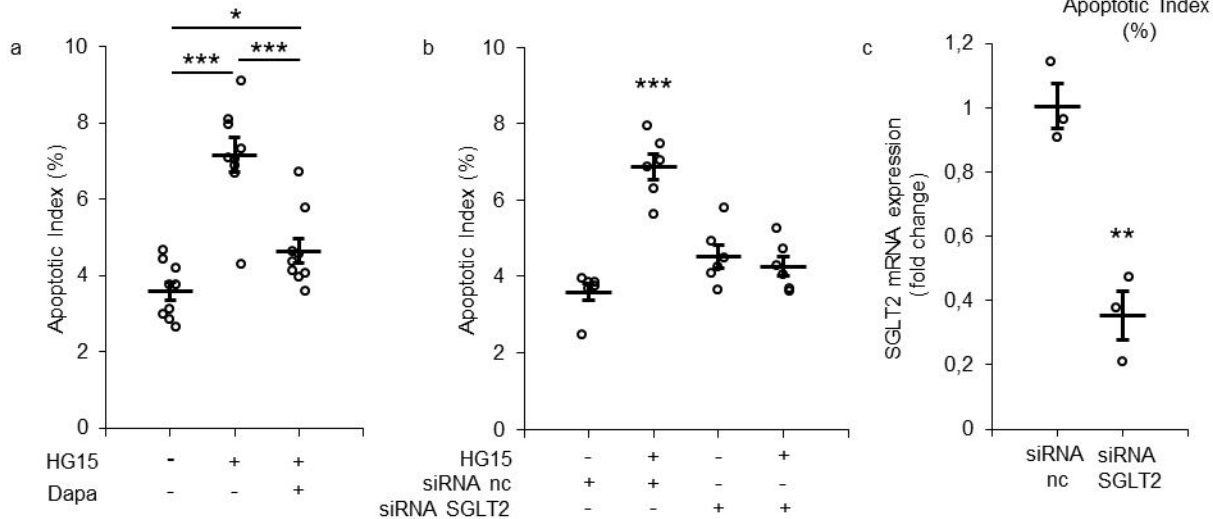
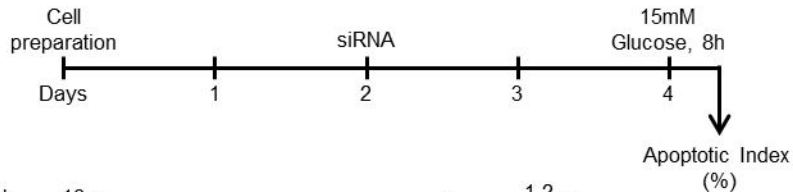
735 **Figure 6. Short-time apoptotic response of MC to increased glucose**
736 **concentration** (a-d) Quantification of AI (a), Bcl-xl abundance (b), Bax abundance
737 (c) and Bax accumulation on mitochondria (d) in MC incubated with control (5.6 mM)
738 or 15 mM glucose containing medium for 8 h. n=12 coverslips from 4 individual cell
739 preparations for AI and Bcl-xl. n=13 coverslips from 5 individual cell preparations for
740 Bax. (e, f) Immunofluorescence staining for Bcl-xl (e) and Bax (f) expression (red) in
741 MC incubated with control or 15 mM glucose containing medium for 8 h.
742 Mitochondria are shown in green. Scale bars 10 μ m. (g) Quantification of AI in MC
743 incubated with control, 15 mM glucose or 15 mM glucose + 0.2 mM phlorizin
744 containing medium for 8 h. Phlorizin was dissolved in DMSO, an equal amount
745 DMSO was added to all samples as control. n=9 coverslips from 3 individual cell
746 preparations. Data are expressed as mean \pm SEM. *p<0.05, **p<0.01, ***p<0.001

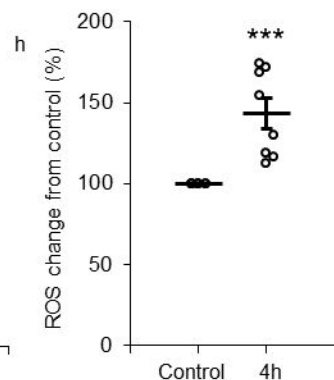
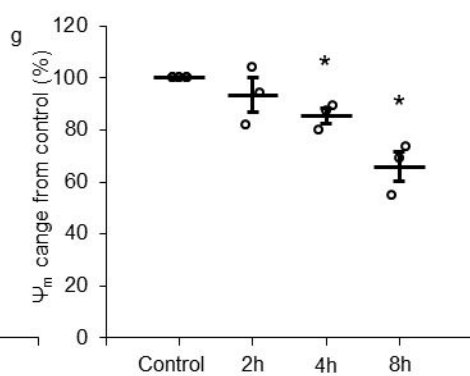
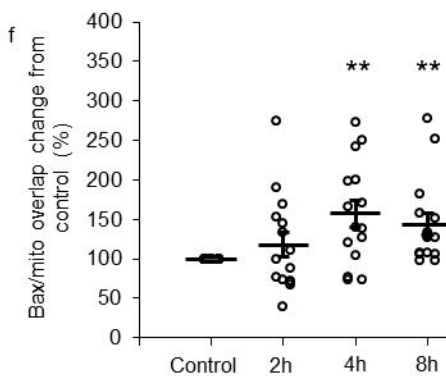
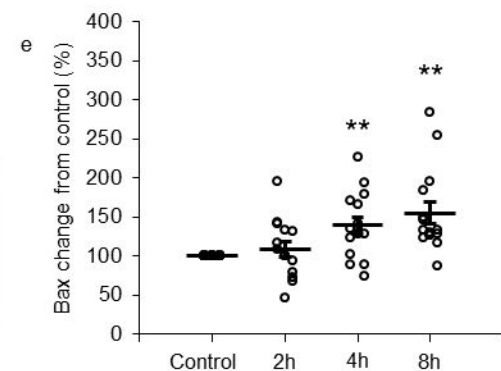
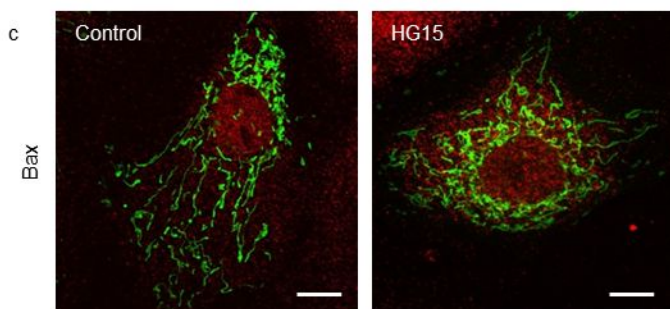
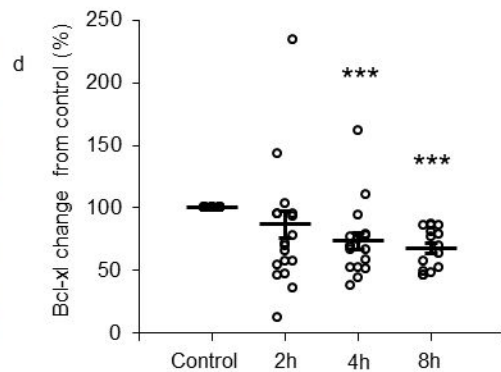
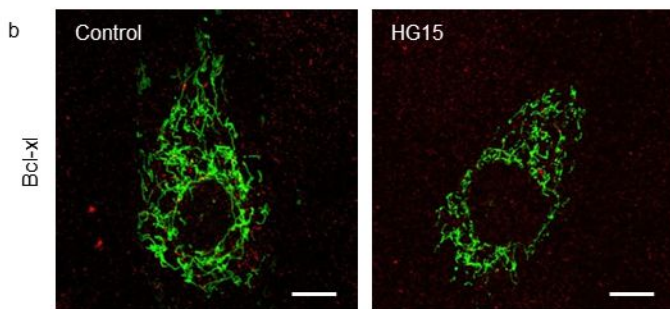
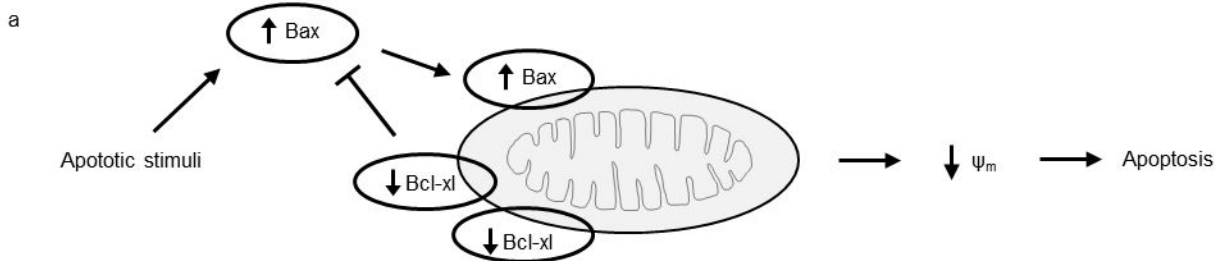
747 **Figure 7. Primary podocytes do not exhibit short-time apoptotic response to**
748 **increased glucose concentration** (a) Immunostaining for podocyte specific markers
749 in primary podocytes; left synaptopodin (green) and DAPI (blue), right nephrin (red)
750 and WT1 (green). Scale bars 10 μm . (b) Quantification of AI in podocytes incubated
751 with control (5.6 mM) or 15 mM glucose containing medium for 8 h. n=12 coverslips
752 from 4 individual cell preparations. (c) Quantification of ROS production in podocytes
753 incubated with control or 15 mM glucose containing medium for 8 h. n=8 coverslips
754 from 2 individual cell preparations. (d, e) Quantification of AI in podocytes incubated
755 with control or 30 mM glucose containing medium for 8 h (d) or 24 h (e). n=12
756 coverslips from 4 individual cell preparations. (f) Podocytes stained with TUNEL
757 (red), WT1 (green) and DAPI (blue). Podocytes were incubated with control, 15 mM
758 glucose or 30 mM glucose for 8 or 24 h as indicated. Scale bars 40 μm . Data are
759 expressed as mean \pm SEM.

760 **Figure 8. Immortalized podocytes transfected with SGLT2 do not have a**
761 **sodium-dependent glucose uptake or increased apoptosis** (a) Immortalized
762 podocytes transfected with SGLT2-ires-CFP (green). Nuclei were counterstained with
763 DRAQ5 (red). Scale bar 40 μm . (b) Immunostaining for SGLT2 (green) in
764 immortalized podocytes transfected with SGLT2. Scale bar 40 μm . (c) Glucose
765 uptake in immortalized podocytes measured with 2-NBDG (green) in Na^+ or Na^+ -free
766 buffer (5.6 mM glucose). Scale bars 40 μm . (d) Quantification of Na^+ -dependent
767 glucose uptake in immortalized podocytes. n=8 coverslips. (e) Quantification of AI of
768 immortalized podocytes transfected with empty vector CFP or SGLT2, incubated with
769 control (5.6 mM) or 15 mM glucose containing medium for 8 h. n=6 coverslips. Data
770 are expressed as mean \pm SEM.

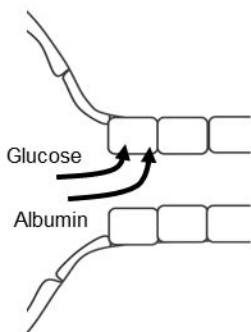




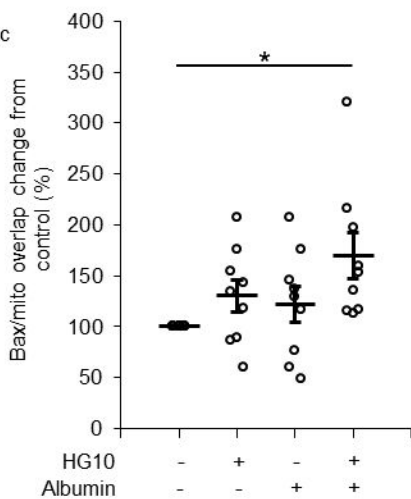




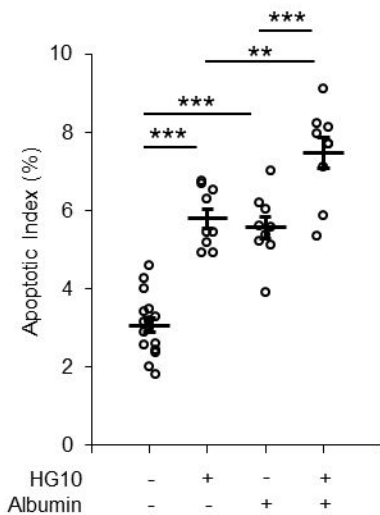
a



c



b



d

